

Controlled Bioactive Nanostructures from Self-Assembly of Peptide Building Blocks**

Yong-beom Lim, Eunji Lee, and Myongsoo Lee*

Molecular self-assembly has become one of the most intensive areas of research during recent years.^[1] This is, in part, due to its vast potential for use in many industrial and biotechnological applications. For biotechnological applications of self-assembled supramolecular nanostructures, the exterior of the nanostructures should be coated with bioactive molecules to construct functional materials. Among many bioactive molecules that could be used, coating of the nanostructures with peptides provides unique opportunities to explore the myriads of biological events that peptides mediate.^[2] The discovery of a general strategy to assemble functional peptides into stable nanostructures with desired size and shape should be one of the most important issues in developing peptide-based self-assembly systems. It can be speculated that the larger and more highly charged peptides demand stronger hydrophobic interactions for stable self-assembly.

Herein, we report on versatile strategies for the self-assembly of any type of large and highly charged peptides and for the control of the sizes and morphologies of peptide-coated nanostructures. To address this, we synthesized a novel class of several supramolecular building blocks which consist of a functional peptide and a hydrophobic lipid dendrimer. As the functional peptide, we selected Tat cell-penetrating peptide (Tat CPP), a well-known CPP from human immunodeficiency virus type-1 (HIV-1).^[3] The 13-mer Tat CPP (Tat₄₈₋₆₀) is a highly charged peptide with 8 positive residues (2 lysines and 6 arginines). One of the advantages of Tat CPP is that it can be translocated efficiently in the cell nucleus, as well as in the cell cytoplasm. Many efforts have been made to utilize Tat CPP for delivering bioactive molecules, either by direct conjugation of the bioactive molecules with Tat CPP or by dendrimer and nanoparticle display of Tat CPP.^[3a-c] Another important biological activity of Tat CPP is that the CPP domain of Tat protein binds specifically to the HIV-1 *trans*-acting response element (TAR) RNA hairpin.^[3d] As binding of Tat protein to viral mRNA at the TAR is essential

for viral transcription and replication, the development of inhibitors of this interaction has been the subject of anti-HIV drug discovery.^[3e]

In the self-assembly of conventional amphiphilic block copolymers, the length and composition of each block affects the stability (aggregation strength), size, and shape of the nanostructures.^[1c-e] To systematically study the effect of the relative composition of the hydrophobic blocks in peptide block molecules on the stability and supramolecular morphology, we dendritically increased the number of lipid molecules (stearic acid, C₁₈) attached to the N terminus of Tat CPP from one to four, thereby yielding TLD-m (monobranched), TLD-d (dibranched), and TLD-t (tetrabranched; Figure 1). The TLDs consist of three blocks, a biofunctional Tat CPP, a flexible linker (ϵ -aminohexanoic acid), and a lipid chain. All of the TLDs were soluble in water.

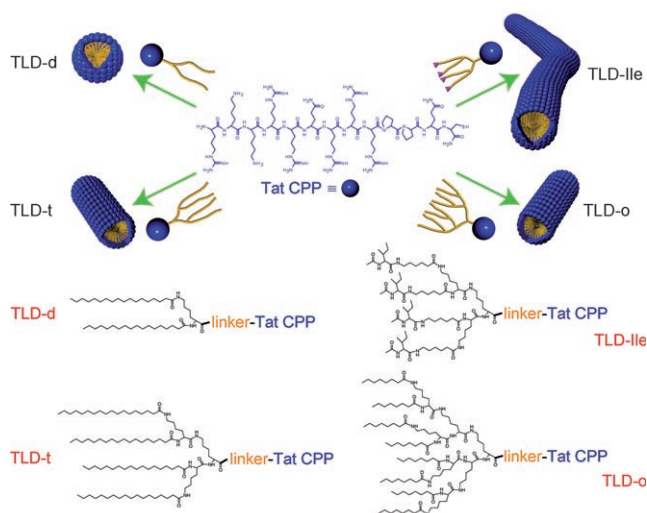


Figure 1. Various morphologies of self-assembled nanostructures formed from Tat-CPP/lipid dendrimers (TLDs). The hydrophobic chain and linker segment of the TLD is shown in yellow. Acetylated isoleucine residues in TLD-Ile are shown as purple triangles. The chemical structures of the hydrophobic chains are presented. For full structures, see the Supporting Information.

To address the question of whether TLD amphiphiles can form supramolecular nanostructures composed of a hydrophobic core of lipids and a hydrophilic corona of Tat CPP in aqueous solution, encapsulation experiments with the hydrophobic dye Nile red were performed. The encapsulation experiments were performed with varying concentrations of TLDs while the Nile red concentration remained unchanged, and the fluorescence emissions of the dye were measured. A

[*] Dr. Y.-b. Lim, E. Lee, Prof. M. Lee
Center for Supramolecular Nano-Assembly and Department of Chemistry
Yonsei University
Seoul 120-749 (Korea)
Fax: (+82) 2-393-6096
E-mail: mslee@yonsei.ac.kr
Homepage: <http://csna.yonsei.ac.kr>

[**] We gratefully acknowledge the National Creative Research Initiative Program of the Korean Ministry of Science and Technology for financial support of this work.

Supporting information for this article is available on the WWW under <http://www.angewandte.org> or from the author.

plot of the emission maximum at 635 nm versus the log of the TLD concentration revealed that there was only a very weak and hardly detectable fluorescence signal when TLD-m was used, a result suggesting that TLD-m did not self-assemble in the range of concentration tested (up to 1 mM). In contrast, inflection points in fluorescence intensity were observed when TLD-d and TLD-t were used, which indicates that these molecules self-assembled above certain threshold concentrations.^[4] The calculated critical micelle concentration (cmc) for TLD-d was 208 μM in pure water, whereas an almost 10 times lower value for the cmc (21 μM) was obtained for TLD-t. The results indicate that only a twofold increase in the number of stearic acids from TLD-d to TLD-t dramatically increases the stability of the nanostructures. A similar dramatic increase in the cmc with an increase in the number of hydrophobic chains has been found with gemini surfactants.^[5] Most biological phenomena take place at very low concentrations; therefore, in many cases it is desirable for the nanostructures to have low cmc values. Besides, if the concentration required to maintain the supramolecular state is too high, there can be cytotoxicity issues. This is also true for Tat CPP, as it has, like other polycations, appreciable cytotoxicity at high concentrations.^[3]

Dynamic light scattering (DLS) examinations revealed that the average hydrodynamic radius (R_H) of the TLD-d supramolecular aggregates is 6.5 nm (Figure 2a). With con-

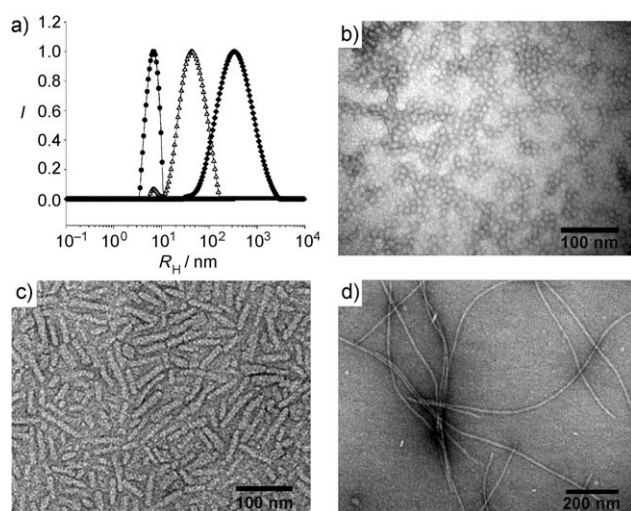


Figure 2. a) Distribution of the hydrodynamic radius (R_H) of TLD-d (\bullet), TLD-t (Δ), and TLD-Ile (\blacklozenge) nanostructures. TEM micrographs of b) TLD-d, c) TLD-t, and d) TLD-Ile nanostructures.

sideration of the extended molecular length of TLD-d (6.2 nm by CPK model), the found R_H value corresponds to that of spherical micelles. In comparison, the average R_H value for TLD-t aggregates was 43 nm (Figure 2a). A small number of TLD-t aggregates with an R_H value of 6.8 nm coexisted with the larger aggregates; this value almost corresponds to the extended molecular length of TLD-t (6.6 nm by CPK modeling). All of the experiments were performed at concentrations above the cmc values. Figure 2b shows a transmission electron microscopy (TEM) micrograph of TLD-d aggregates. The micrograph revealed that TLD-d formed spherical

micelles of approximately 11 nm in diameter, which is in line with the DLS data. The small difference in the aggregate size between the DLS and TEM data (13 versus 11 nm) is likely due to the fact that the Tat-CPP chain is hydrated under the DLS solution conditions, whereas the sample is in the dried state during TEM. A TEM investigation of TLD-t showed that most of the TLD-t nanostructures existed as short-length cylindrical micelles of approximately 12 nm in diameter and with an average length of approximately 100 nm, together with a very small population of spherical micelles (Figure 2c). This result correlates well with the DLS data of TLD-t. Therefore, it can be concluded that the bigger nanostructures with a radius of 43 nm in the DLS examination correspond to the short-length cylindrical micelles, while the smaller nanostructures correspond to the spherical micelles. The results suggest that the short-length cylindrical micelles might be formed through spherical micelles as intermediate structures. The supramolecular morphologies of the TLDs agree well with the theory that the morphology of amphiphiles is directed by the hydrophilic-to-hydrophobic ratio.^[1c-e] It should be noted that the nanostructure formation was instantaneous and prolonged storage of up to several months did not change the size and shape of the nanostructures.

Investigations of the Tat-CPP secondary structure in the supramolecular nanostructures of TLD-d and TLD-t by circular dichroism (CD) spectroscopy revealed that the peptides adopted random-coil structures.^[4] It is well known that Tat CPP forms a random-coil structure when it exists as an isolated peptide in solution.^[3d] This evidence indicates that there is no hydrogen bonding, such as β -sheet interactions, among the peptide segments. Therefore, the hydrophobic interactions among the phase-separated lipid blocks are the sole driving force for the self-assembly of the TLDs; from this, it can be interpreted that the Tat CPP does not take part in the self-assembly process and retains its biological activity.

We next asked whether we can have another level of control over the supramolecular morphology of the Tat-CPP-coated nanostructures. For this, we synthesized TLD-o, with twofold more branches (octabranch) than TLD-t, while maintaining the volume fraction of the hydrophobic segment by using a shorter lipid chain (octanoic acid, C_8). TLD-o formed short-length cylindrical micelles similarly to TLD-t ($R_H = 5.1$ and 56 nm for the smaller and larger aggregates, respectively).^[4] The size of the nanostructures measured from DLS and TEM data correlated well with the molecular dimensions of TLD-o. Likewise, the introduction of nonanoic acid (C_9) resulted in the formation of short-length cylindrical micelles (data not shown).

The reason why the growth of cylindrical nanostructures of TLD-t and TLD-o terminates at an early stage of self-assembly to form short-length cylindrical micelles is not clear at this point. At present, we hypothesize that the dendrimer architecture and the resulting unique close packing of the lipid chains might be responsible for this. To investigate how disruption in the close packing of the lipid chains affects the self-assembly behavior of the TLDs, we designed TLD-Ile which contains chiral and hydrophobic isoleucine amino acids at the distal end of the lipid chains (Figure 1). Interestingly,

investigation by DLS and TEM revealed that TLD-Ile formed bigger nanostructures ($R_H = 340$ nm) than other TLDs, and the nanostructures had long-length cylindrical micelle morphology (Figure 2 a and d). The result indicates that incorporation of molecules of dissimilar structure, such as chiral amino acids, into the hydrophobic lipid chains can induce different types of supramolecular packing. Hydrogen bonding between the isoleucines may also be a contributory factor. It would be interesting to systematically investigate how the morphology of TLDs can be further controlled by introducing other types of dissimilar structures or amino acids other than isoleucine into the lipid block; this will be the subject of future study.

The short-length cylindrical micelles might be useful for efficient intracellular delivery applications due to their small size and multivalent Tat CPP coating. Block molecules having amphiphilic character can form core-shell-type micelles and have long been explored for drug-delivery applications, with the encapsulation of hydrophobic drugs in the core.^[6] To investigate the possibility of using the Tat-CPP-coated nanostructures for drug-delivery applications, we first measured the cytotoxicity of the TLDs (Figure 3 a). TLD-d was found to

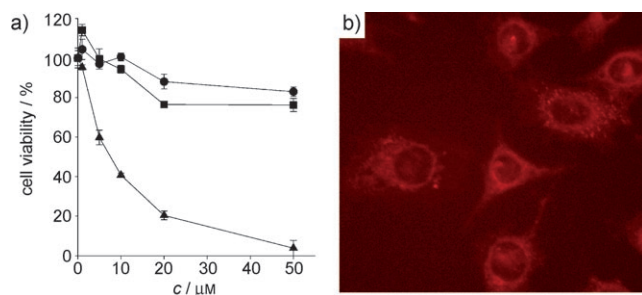


Figure 3. a) Cytotoxicity in HeLa cells by MTT assay for Tat CPP (●), TLD-t (■), and TLD-d (▲). Mean values \pm standard deviation are shown ($n=3$). b) Confocal laser scanning microscopy (CLSM) image ($400\times$) of intracellular delivery of Nile red by TLD-t short-length cylindrical micelles. The TLD-t concentration was $10 \mu\text{M}$ and the amount of encapsulated Nile red was 3 mol% relative to TLD-t. The cells were treated for 3 h.

be highly cytotoxic. When the cells were incubated with TLD-d, the plasma membranes disappeared, a result indicating that cell lysis had occurred. This result suggests that TLD-d nanostructures disintegrate and/or exist as isolated molecules during interaction with the plasma membrane due to their weak association strength, thereby lysing cell membranes in a similar manner to conventional surfactants. In contrast, the cytotoxicity of TLD-t was similar to that of unimolecular Tat CPP; this suggests that TLD-t nanostructures are stable enough to maintain their self-assembled state during cell internalization. It has previously been discussed that stable molecular assembly prevents free diffusion of the individual amphiphilic components to the cell surface.^[7]

The loading-capacity measurement revealed that 4.2 mol% of Nile red molecules are encapsulated relative to TLD-t.^[4] The loading capacity may be further optimized by varying many parameters of the encapsulation experiment. TEM investigation of TLD-t nanostructures loaded with Nile

red showed that the short-length cylindrical micelle morphology is essentially unchanged even after encapsulation of the guest molecules.^[4]

Intracellular delivery experiments with TLD-t encapsulating Nile red showed that the delivery was very efficient, with every cell being brightly fluorescent after treatment (Figure 3 b and Figure S8 in the Supporting Information). The guest molecules were even effectively translocated into the nucleus. These results indicate that the cargo-unloading process is efficient in the cytoplasm, while some TLD-t nanostructures that remain intact and/or are only partially disintegrated in the cytoplasmic compartment enter the nucleus through the nucleus-localization activity of Tat CPP. The small size of the TLD-t nanostructures and the multivalent presentation^[3b,8] of Tat CPP are likely to be the reasons for this efficient cell delivery activity.

We have shown that the dendrimerization of a lipid block is a versatile way of controlling the size, shape, and aggregation strength of amphiphilic peptide block molecules. This approach might be applied to any type of hydrophilic peptides, thereby making it possible to explore a myriad of peptide-mediated biological phenomena. In addition, the notable feature of the Tat peptide nanostructures is their ability to efficiently deliver encapsulated guest molecules into both the cytoplasmic and nucleus compartments. The nucleus is the site of action for many drugs and most anticancer drugs. We have previously shown that hydrophobic molecules, when encapsulated in Tat-CPP-coated β -sheet nanoribbons, are released predominantly in the cytoplasmic compartment.^[9] These collective findings suggest that hydrophobic-interaction-mediated TLD nanostructures might be more stable than the β -sheet-mediated ribbon nanostructures in the cytoplasmic compartment.

Received: June 21, 2007

Published online: October 19, 2007

Keywords: dendrimers · nanomaterials · peptides · self-assembly · supramolecular chemistry

- [1] a) J.-M. Lehn, *Proc. Natl. Acad. Sci. USA* **2002**, *99*, 4763–4768; b) L. Brunsveld, B. J. B. Folmer, E. W. Meijer, R. P. Sijbesma, *Chem. Rev.* **2001**, *101*, 4071–4097; c) T. Shimizu, M. Masuda, H. Minamikawa, *Chem. Rev.* **2005**, *105*, 1401–1443; d) M. Lee, B.-K. Cho, W.-C. Zin, *Chem. Rev.* **2001**, *101*, 3869–3892; e) D. E. Discher, A. Eisenberg, *Science* **2002**, *297*, 967–973; f) J. A. A. W. Elemans, A. E. Rowan, R. J. M. Nolte, *J. Mater. Chem.* **2003**, *13*, 2661–2670; g) K. Kinbara, T. Aida, *Chem. Rev.* **2005**, *105*, 1377–1400; h) A. Mueller, D. F. O'Brien, *Chem. Rev.* **2002**, *102*, 727–757; i) D. Chen, M. Jiang, *Acc. Chem. Res.* **2005**, *38*, 494–502; j) J.-H. Ryu, E. Lee, Y.-b. Lim, M. Lee, *J. Am. Chem. Soc.* **2007**, *129*, 4808–4814.
- [2] a) S. Zhang, *Nat. Biotechnol.* **2003**, *21*, 1171–1178; b) R. J. Mart, R. D. Osborne, M. M. Stevens, R. V. Ulijn, *Soft Matter* **2006**, *2*, 822–835; c) R. Langer, D. A. Tirrell, *Nature* **2004**, *428*, 487–492; d) G. A. Silva, C. Czeisler, K. L. Niece, E. Beniash, D. A. Harrington, J. A. Kessler, S. I. Stupp, *Science* **2004**, *303*, 1352–1355; e) M. M. Stevens, N. T. Flynn, C. Wang, D. A. Tirrell, R. Langer, *Adv. Mater.* **2004**, *16*, 915–918; f) J. Hentschel, E. Krause, H. G. Börner, *J. Am. Chem. Soc.* **2006**, *128*, 7722–7723; g) M. R. Ghadiri, J. R. Granja, R. A. Milligan, D. E. McRee, N. Khazano-

- vich, *Nature* **1993**, 366, 324–327; h) S. Ghosh, M. Reches, E. Gazit, S. Verma, *Angew. Chem.* **2007**, 119, 2048–2050; *Angew. Chem. Int. Ed.* **2007**, 46, 2002–2004; i) E. P. Holowka, V. Z. Sun, D. T. Kamei, T. J. Deming, *Nat. Mater.* **2007**, 6, 52–57; j) Y.-b. Lim, S. Park, E. Lee, H. Jeong, J.-H. Ryu, M. S. Lee, M. Lee, *Biomacromolecules* **2007**, 8, 1404–1408.
- [3] a) S. Futaki, *Adv. Drug Delivery Rev.* **2005**, 57, 547–558; b) M. Sung, G. M. K. Poon, J. Gariépy, *Biochim. Biophys. Acta Biomembr.* **2006**, 1758, 355–363; c) S. R. Schwarze, A. Ho, A. Vocero-Akbani, S. F. Dowdy, *Science* **1999**, 285, 1569–1572; d) A. D. Frankel, *Curr. Opin. Struct. Biol.* **2000**, 10, 332–340; e) C. U. Dinesh, T. M. Rana in *Small molecule DNA and RNA binders* (Eds.: M. Demeunynck, C. Bailly, W. D. Wilson), Wiley-VCH, Weinheim, **2003**, pp. 58–87.
- [4] See the Supporting Information.
- [5] F. M. Menger, J. S. Keiper, *Angew. Chem.* **2000**, 112, 1980–1996; *Angew. Chem. Int. Ed.* **2000**, 39, 1906–1920.
- [6] a) H. Otsuka, Y. Nagasaki, K. Kataoka, *Adv. Drug Delivery Rev.* **2003**, 55, 403–419; b) R. Haag, F. Kratz, *Angew. Chem.* **2006**, 118, 1218–1237; *Angew. Chem. Int. Ed.* **2006**, 45, 1198–1215; c) R. Savić, L. Luo, A. Eisenberg, D. Maysinger, *Science* **2003**, 300, 615–618.
- [7] L. M. Pakstis, B. Ozbas, K. D. Hales, A. P. Nowak, T. J. Deming, D. Pochan, *Biomacromolecules* **2004**, 5, 312–318.
- [8] a) Y.-b. Lim, M. Lee, *Org. Biomol. Chem.* **2007**, 5, 401–405; b) M. Mammen, S. K. Choi, G. M. Whitesides, *Angew. Chem.* **1998**, 110, 2908–2953; *Angew. Chem. Int. Ed.* **1998**, 37, 2754–2794; c) C. R. Bertozzi, L. L. Kiessling, *Science* **2001**, 291, 2357–2364.
- [9] Y.-b. Lim, E. Lee, M. Lee, *Angew. Chem.* **2007**, 119, 3545–3548; *Angew. Chem. Int. Ed.* **2007**, 46, 3475–3478.
-